Finite element models for the study of hydrogen embrittlement of steel structures

Daniella LOPES PINTO [1,2*]
daniella.lopes_pinto@minesparis.psl.eu

Academic advisor: Jacques BESSON [1]

Industrial advisors: Nikolay OSIPOV [2]

[1] Centre des Matériaux, Mines Paris

[2] Transvalor S.A.

Thesis defense
March 7th 2025

- In the context of **energy transition**, **hydrogen** plays an important role as an **energy vector**
- Hydrogen can be produced from other **renewable sources**, such as wind and solar
- Hydrogen transport using **existing natural gas pipelines** (40,000 km in France, 50 billion in assets, up to 80 years old) is a proposal for hydrogen transport

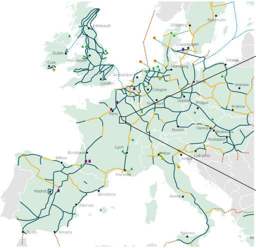

Background and challenges

- The steels used in gas pipelines are typically susceptible to **hydrogen embrittlement**
- Hydrogen embrittlement: ductility and toughness reduction, premature failure
- **Measure material properties from small samples without service interruption**

Coupon extracted from the pipeline

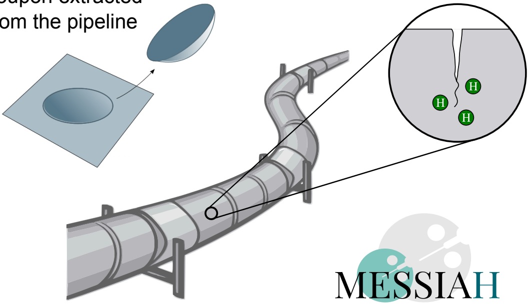

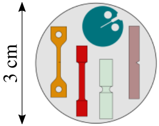

MESSIAH
Chaire ANR industrielle

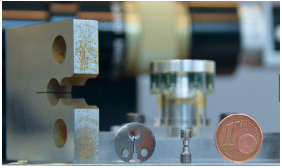

Background and Challenges

- Experimental observations show that **toughness decreases with increasing specimen thickness** until reaching a plateau
- Beyond a critical thickness, toughness becomes relatively insensitive to further increases

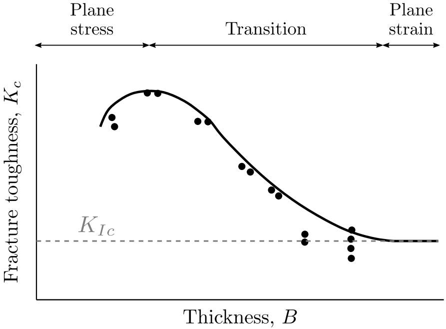

Adapted from Barsom and Rolfe, 1987.

Objectives

- Develop a model coupling **plasticity**, **damage**, and **hydrogen diffusion**
- Validate the model against experimental data
- Simulate size and thickness effects on toughness using sub-size specimens

- **Introduction**
- **Hydrogen inside metals**
- **Finite element formulation**
- **Numerical simulations**
  - Pressurized disks tests
  - Hydrogen uptake during a tensile test
  - Hydrogen embrittlement modeling
  - Simulation of fracture toughness tests
- **Conclusions and perspectives**

Outline

Hydrogen uptake

- **Sieverts' law:** The solubility of a diatomic gas in a metal is proportional to the square root of the gas pressure

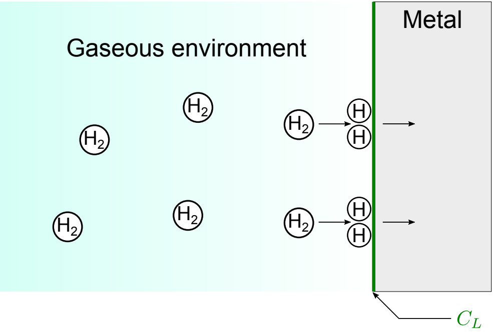

Thermally activated term

$$C_L = \gamma\sqrt{P_a}$$

Hydrogen solubility (H at./ Iron at.)

H_2 pressure (MPa)

MINES PARIS | PSL

- Model from Sofronis and McMeeking (1989) and corrected by Krom *et al.* (1999)

- **Hydrogen concentration:** $C = C_L + C_T$
  - Lattice concentration: $C_L = \beta N_L \theta_L$
  - Trapped concentration: $C_T = \sum_i^N C_T^i = N_T^i(\kappa)\theta_T^i$

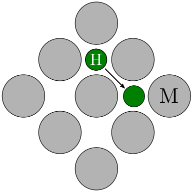

- **Hydrogen flux:**

$$J = -D_L \nabla C_L + \frac{D_L C_L V_H}{RT} \nabla p$$

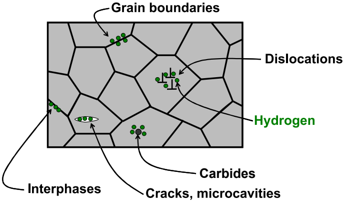

- **Oriani's equilibrium:**

$$\frac{1-\theta_L}{\theta_L} \frac{\theta_T^i}{1-\theta_T^i} = K$$

(Coupling terms)

Material damage

- The **ductile behavior** of the metal is described by the **GTN model** (Tvergaard *et al.* 1984):

$$\frac{\sigma_{eq}^2}{\sigma_F^2} + 2q_1 f_* \cosh\left(\frac{q_2}{2}\frac{\sigma_{ii}}{\sigma_F}\right) - 1 - q_1^2 f_*^2 = 0$$

$$\dot{f} = \dot{f}_{nucleation} + \dot{f}_{growth}$$

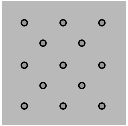

Impurities or second phase particles

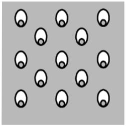

Void nucleation and growth

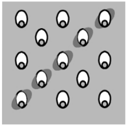

Strain localization

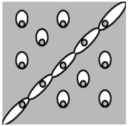

Void coalescence and fracture

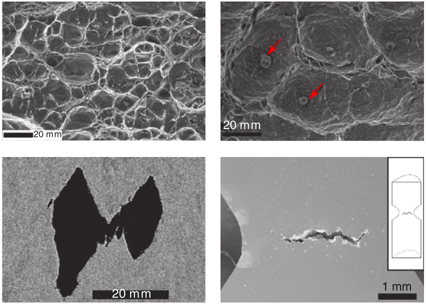

- **Void growth**: Unchanged due to mass conservation

$$\dot{f}_g = (1 - f_g)\mathrm{trace}(\dot{\varepsilon}_p)$$

- **Void nucleation**: Proposed dependance on hydrogen concentration

$$\dot{f}_n = A_n(\kappa)\dot{\kappa} + B_n(C)\dot{\kappa}$$

(Coupling terms)

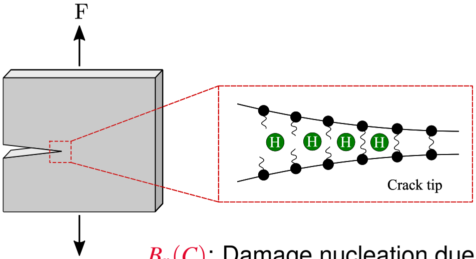

Hydrogen weakens the cohesive bonds between atoms

$B_n(C)$: Damage nucleation due to hydrogen
HEDE (Hydrogen Enhanced Decohesion)

Outline

Mixed formulation

- Fully implicit finite strain framework
- Based on a mixed formulation: $\underline{u}, P, \theta$ (Zhang *et al.* 2017) and C_L
- Quadratic elements with reduced integration
- **Aim:** better pressure fields by avoiding volumetric locking

Advantage

∇p can be directly computed from nodal values

$$J = -D_L \nabla C_L + \frac{D_L C_L V_H}{RT} \nabla p$$

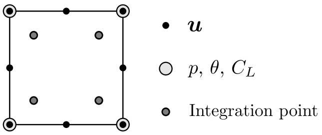

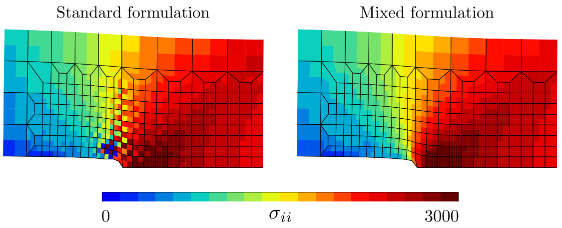

$\boldsymbol{B}$-bar formulation

- The use of **quadratic elements** with additional dofs lead to **high simulation times**
- $\boldsymbol{B}$-bar (or $\bar{\boldsymbol{B}}$) formulation (Hughes, 1980):
  - Linear elements with full integration
  - Solves volumetric locking by modifying the strain-displacement matrix:

$$\bar{\boldsymbol{B}} = \boldsymbol{B}_d + \bar{\boldsymbol{B}}_h$$

  - To avoid extrapolating p to the nodes for ∇p computation, it is considered as a dof

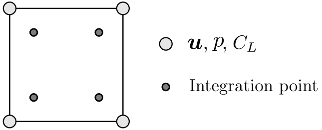

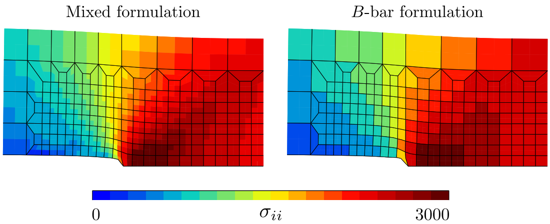

B-bar formulation

- Test on a Disk Compact Tension (DCT) specimen with 5200 elements:
  - **Mixed formulation**: 103,762 dofs, 1h 40 minutes to complete
  - ***B*-bar formulation**: 33,974 dofs, 18 minutes to complete

- Slightly higher force for the B-bar formulation $\rightarrow$ Linear elements are inherently stiffer since they have less nodes

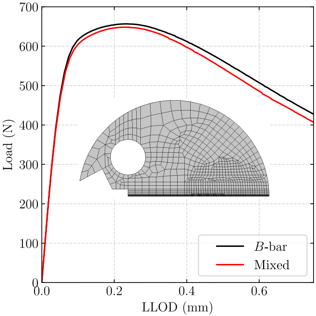

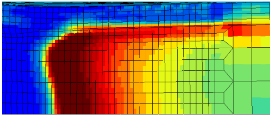

Mixed formulation

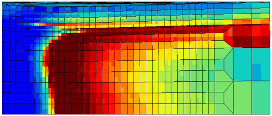

B-bar formulation

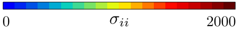

Nonlocal damage model

- Damage models such as the GTN model are known to induce **spurious mesh dependency** (element size, type and orientation)
- To solve this problem, it is proposed to use a **nonlocal damage model** based on the **implicit gradient** by Peerlings *et al.*, 1996

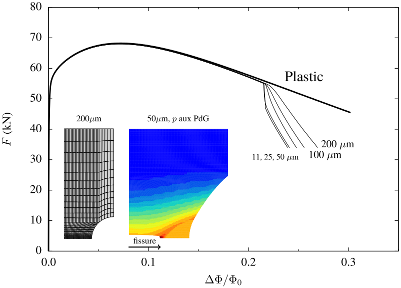

Notched tensile (NT) specimen

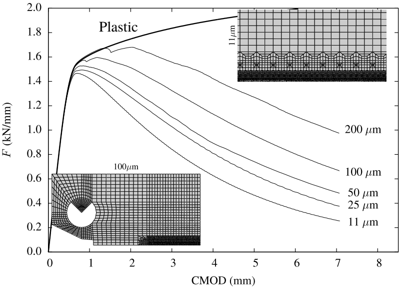

Compact tension (CT) specimen

(Besson, 2021)

Nonlocal damage model

- Two variables are used (two associated internal lengths: $\bar{\omega}$ and $\bar{\kappa}$):
  - **Plastic volume variation:** $\bar{\omega} - \ell_{\omega}^2 \Delta \bar{\omega} = \omega$ where $\omega = \mathrm{trace}(\dot{\underset{\sim}{\varepsilon}}_p)$
  - **Accumulated plastic strain:** $\bar{\kappa} - \ell_{\kappa}^2 \Delta \bar{\kappa} = \kappa$
- The modified evolution laws for the damage variables are now:
  - **Void growth:** $\dot{f}_g = (1 - f_g)\dot{\bar{\omega}}$
  - **Void nucleation:** $\dot{f}_n = A_n \dot{\bar{\kappa}} + B_n(C)\dot{\bar{\kappa}}$

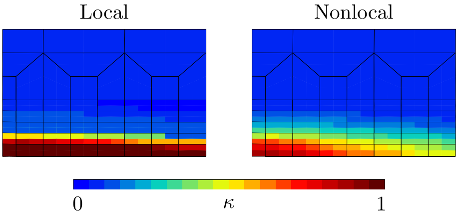

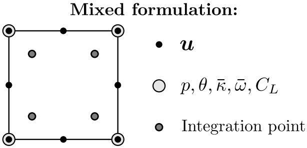

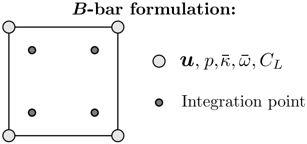

Outline

Context

- **ISO 11114-4 standard:** uses pressurized disk tests for selecting metallic materials resistant to hydrogen embrittlement
- Disk often fails in the clamping zone
- **First step:** redesigning the disk geometry to control failure location

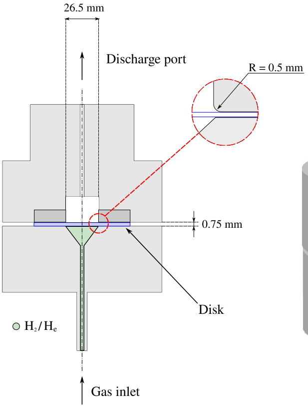

$$\mathrm{HEI} = \frac{P_r(\mathrm{He})}{P_r(\mathrm{H_2})}$$

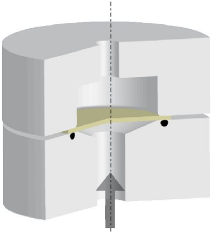

Disk specimen:

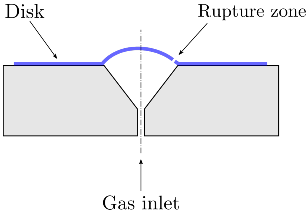

Redesign of the disk geometry

- New proposed geometries:
  - No need to modify the test setup
  - Keep the same minimum thickness of the standard (0.75 mm)
- Optimization with respect to ℓ, R and R' with FE simulations considering an elasto-plastic behavior

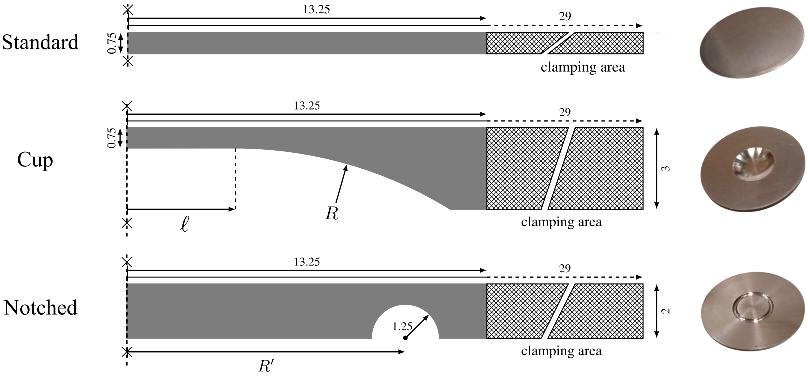

Redesign of the disk geometry

- The location of the maximum accumulated plastic strain (κ) corresponds to the failure location

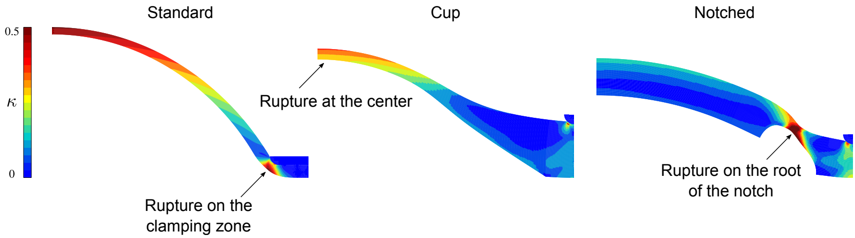

Materials

- **X52 vintage steel:**
  - Yield strength: 400 MPa
  - Different elongation at rupture in T and L directions
- **E355 mod. steel:**
  - Yield strength: 330 MPa
  - Higher elongation at rupture and lower Ultimate Tensile Strength in relation with the vintage material
  - Similar elongation at rupture in both directions
- Elasto(visco)-plastic model coefficients' identified through optimization:

$$\sigma_F(p) = \max(\sigma_L, \sigma_0 + Q_1(1-\exp(-b_1 p)) + Q_2(1-\exp(-b_2 p)) + Hp)$$

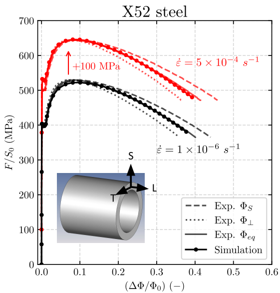

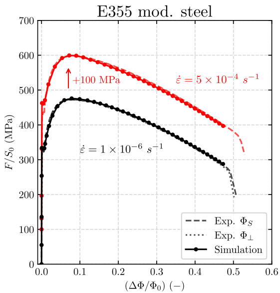

Simulation of pressurized disks

- Axisymmetric model, quadratic elements with reduced integration (mixed formulation)
- Hydrogen diffusion parameters taken from the literature
- Since damage is not considered into the numerical model, the simulations were stopped once they reached experimentally observed rupture pressure (P_r)
- Model's boundary conditions:

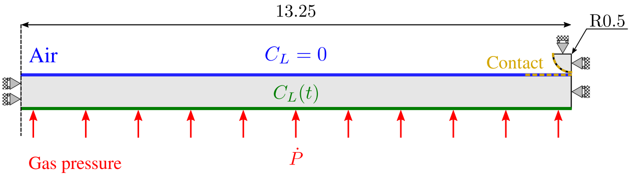

- Experiments carried out by Luciano Santana
- Successfully modification of fracture location
- Failure is primarily driven by plasticity and occurs under a limit load scenario

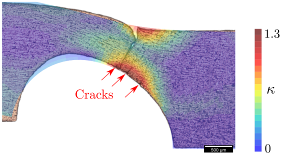

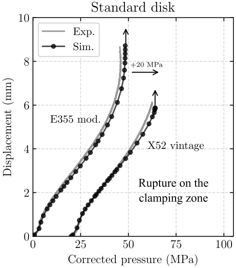

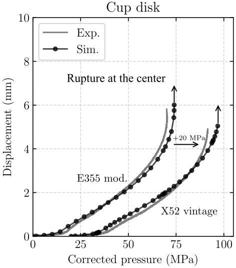

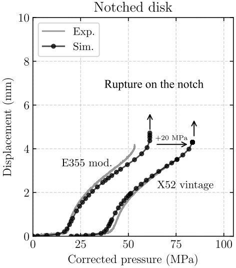

Results under hydrogen (E355 mod. steel)

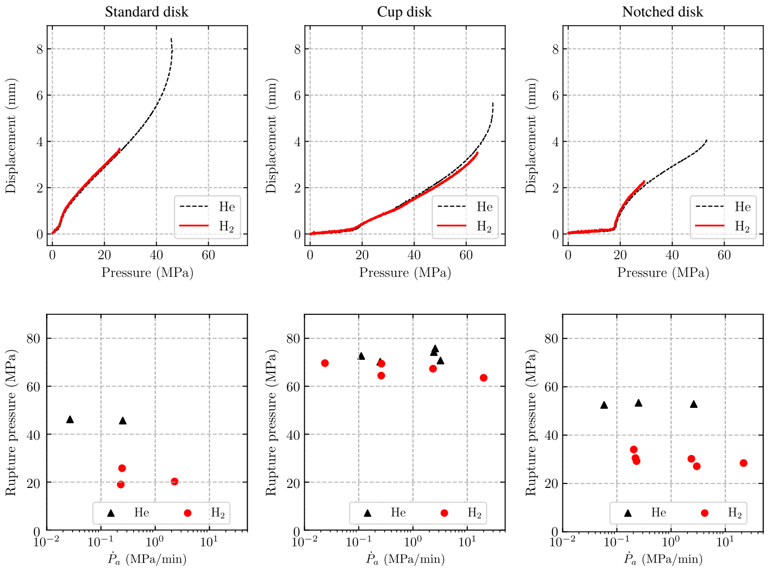

Hydrogen embrittled depth

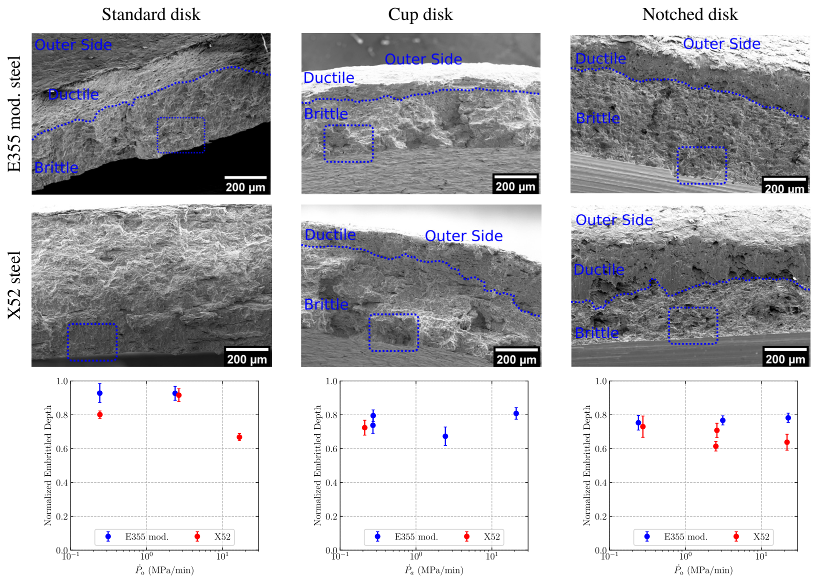

- Considers only one kind of trap: dislocations
- Trap binding energies (W_B) and trap densities (N_T) were taken from the literature and analyzed based on the experimental observations
- Based on the models proposed by Moro *et al.* (2010) and Kumnick *et al.* (1980), four cases emerge

$$W_B = \begin{cases} 40 \ \mathrm{kJ/mol} \\ 60 \ \mathrm{kJ/mol} \end{cases}$$

$$N_T = \begin{cases} \log_{10} N_T = 24.73 - 3.74 \exp(-60.17\kappa) \\ \log_{10} N_T = 23.26 - 2.33 \exp(-5.5\kappa) \end{cases}$$

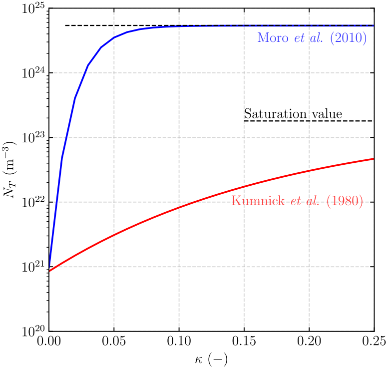

MINES PARIS | PSL

	$\dot{P} = 0.25$ MPa/min	$\dot{P} = 25$ MPa/min	C_{max} (appm)
$W_B = 40$ kJ/mol N_T from Moro *et al.*	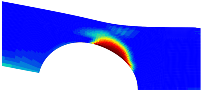	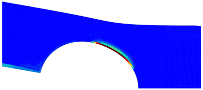	16
$W_B = 40$ kJ/mol N_T from Kumnick *et al.*	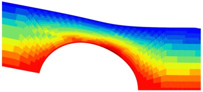	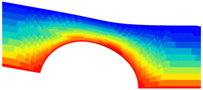	0.3
$W_B = 60$ kJ/mol N_T from Moro *et al.*	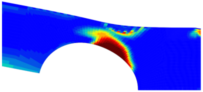	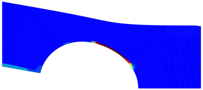	60
$W_B = 60$ kJ/mol N_T from Kumnick *et al.*	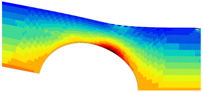	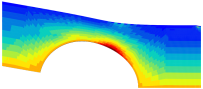	0.4

Principal stress evolution

- Specimens that develop higher principal stress (σ_I) in the fracture zone fail at a lower hydrogen pressure ($P_a(H_2)$)
- The total hydrogen concentration reduces the maximum principal stress that that triggers fracture

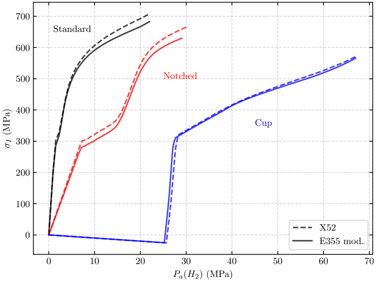

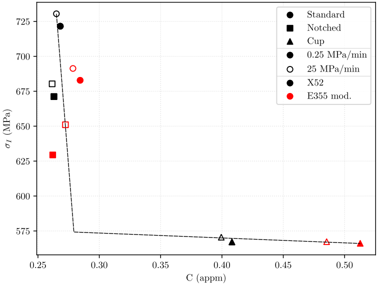

Outline

Tensile test:

- Material: X52 vintage steel
- Gaseous atmosphere under different conditions:

Environment	Air, 85 bar H_2
Strain	0%, 30%Rp02, 90%Rp02, 3%, 6%, 12%
Strain Rate (s^{-1})	1×10^{-5}, 1×10^{-4}, 1×10^{-3}
Dwell	No dwell, Dwell

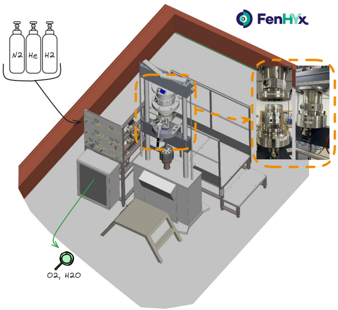

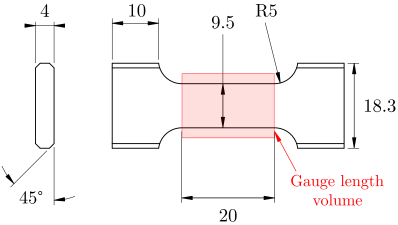

Thermal Desorption Spectroscopy (TDS) test:

- High precision (10^{-3} wppm), calibration with a Certified Reference Material (CRM) with a known hydrogen mass
- Temperature ramp of 10°C/min up to 600°C
- The hydrogen content is determined by integrating the first peak in the TDS spectra

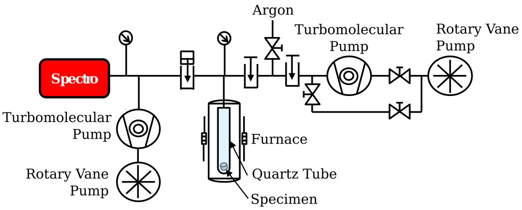

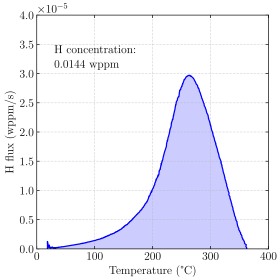

Simulation model

- 3D mesh of 1/8 of the specimen (plane strain)
- Elasto(visco)-plastic behavior
- Hydrogen applied to the exposed surfaces
- $N_T(\kappa)$ adjusted based on experimental results at different strain levels

Displacement boundary conditions:

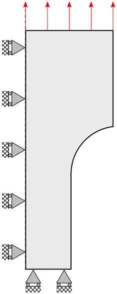

Hydrogen boundary conditions:

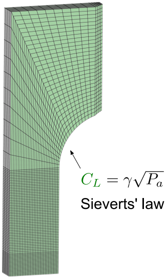

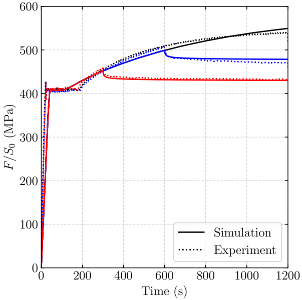

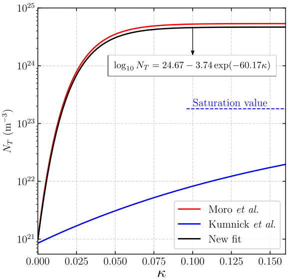

Strain effect

- Specimens deformed up to 90%Rp02, 3%, 6% and 12% at $\dot{\varepsilon} = 1 \times 10^{-4}$ s^{-1}
- Higher strain levels lead to higher hydrogen concentrations
- Most of hydrogen is located at the gauge length
- For all cases, hydrogen is mostly located near the surface

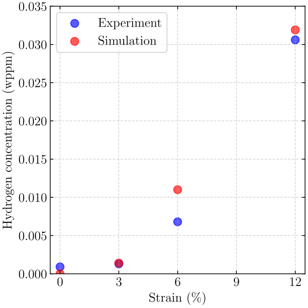

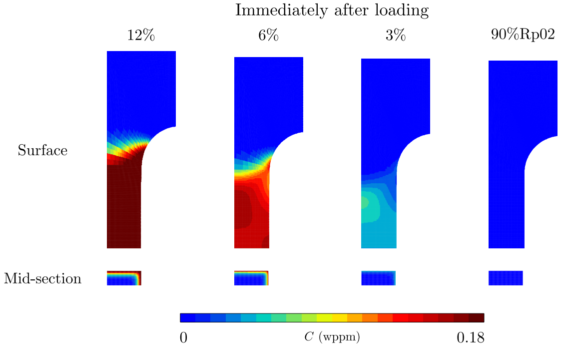

Strain effect

- The preparations required before the TDS test takes approximately **one hour**, at which hydrogen can freely desorb the specimen
- The amount of hydrogen that leaves the specimen during resting is lower at higher strains
- With the actual model, at least 80% of the hydrogen content leaves the specimen during resting

Strain (%)	H concentration before 1h resting (wppm)	H concentration after 1h resting (wppm)	H remaining (%)
12	0.1562	0.0319	20.46
6	0.0797	0.0110	13.80
3	0.0307	0.0014	4.56
90%Rp02	0.0051	0.0000	0.00

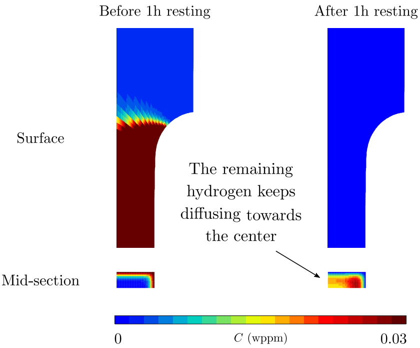

Strain rate effect

- Tests conducted at three different strain rates: 1×10^{-3}, 1×10^{-4} and 1×10^{-5} s^{-1}
- One-hour resting time allowing hydrogen desorption is considered
- **Lower strain rates** lead to **higher hydrogen content**, as hydrogen has more time to diffuse throughout the material

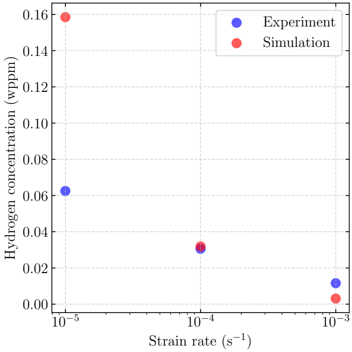

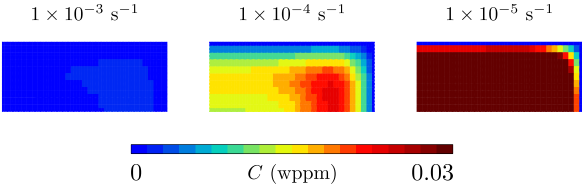

Dwell effect

- **Dwell time:** the time a specimen is exposed to hydrogen without further deformation until it reaches the same exposure time as the most deformed specimen (12%)
- Specimens deformed up to 3% strain at 1×10^{-4} 1×10^{-5} s^{-1}
- Longer exposure $\rightarrow$ Higher hydrogen content

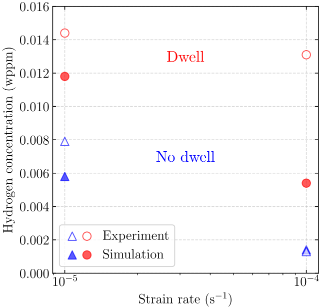

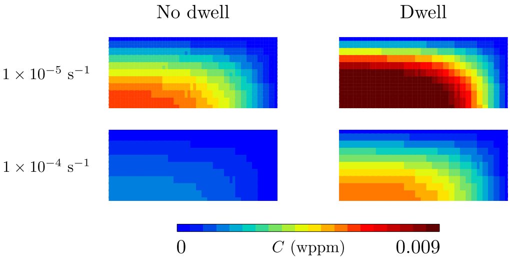

Outline

Outline

Outline

Thank you

Daniella LOPES PINTO
daniella.lopes_pinto@minesparis.psl.eu